Vibrational Studies of the Cluster Carbonyls of Ruthenium and Osmium. Part 2.[1] Single-crystal Raman and Infrared Data for $[Ru_3(CO)_{12}]$ in the CO Stretching Region

Trevor R. Gilson * and, in part, John Evans
Department of Chemistry, The University, Southampton SO9 5NH

Single-crystal Raman and i.r. data are used to give a complete assignment of the crystal modes of $[Ru_3(CO)_{12}]$. The results are definitive in so far as the complex molecule retains its D_{3h} vibrational identity in the crystal. They are used to confirm the solution assignments, and the validity of the oriented gas-phase approximation for complex molecules is discussed.

In Part 1 [1] we attempted to complete the vibrational characterisation of several cluster carbonyls in solution, in the carbonyl stretching region. With crystalline materials, Raman sensitivity is much increased. Whilst the bands sharpen considerably, low site and crystal symmetry allow a substantial departure from ideal vibrational behaviour. In this paper we make a detailed examination of one of the crystalline compounds, $[Ru_3(CO)_{12}]$. Since there is no great likelihood of being able to relate the vibrational perturbations quantitatively to the parameters of solid-state physics or chemistry, we define a series of more pragmatic aims: (*i*) further assistance in assignment of the solution spectra; (*ii*) a general enquiry into the validity of the oriented gas-phase approximation [2] for such a complicated molecule; (*iii*) insight into the particular behaviour of cluster carbonyls in sites of low symmetry.

The first step is to establish the idealised molecular modes from which each crystal mode originates, bearing in mind that there need not be an absolute answer: some modes may be so mixed as to lose their unique identity. The crystal structure of $[Ru_3(CO)_{12}]$ [3] (Figure 1) is particularly interesting in pursuit of these aims, since the molecules are on sites of no symmetry, yet all the molecular M_3 planes are aligned. Indeed, the monoclinic crystals may be considered optically orthorhombic, in the sense that the extinction directions not determined by crystal symmetry remain parallel and perpendicular to the molecular M_3 planes.

Infrared Studies.—No technique has yet been devised for producing thin films of fragile crystals, so that reflectance methods were required.

The interpretation of reflectance data is not straightforward, particularly where broad reflectance bands are observed. The complex nature of the effects is well illustrated in Figure 2(*a*)—(*c*), showing the {001} face spectrum in natural and polarised light. So far from being the sum of the two polarisations, the unpolarised spectrum shows a dramatic change in band profile for the higher frequency region. Similar effects were observed when a micro-reflectance unit was used; confusingly, the less ' pure ' spectra exhibit sharper maxima.

The spectra observed here are not so broad that using reflectance maxima is likely to cause much error in frequency. In accordance with the results obtained from dispersion analysis in simpler cases,[4] high-frequency ill resolved shoulders are ignored.† Low-frequency shoulders are treated less circumspectly. The results are consistent with the Raman spectra (Table 1), in the sense that g/u correlation splittings are limited to a few cm^{-1} only, and no larger than the a_u/b_u and a_g/b_g splittings observed in the i.r. or Raman spectra.

† We note particularly the 2 072 cm^{-1} shoulder found by Adams and Taylor,[5] quite unresolved in our best spectra, which separates in varying degree with convergent light or impure polarisation.

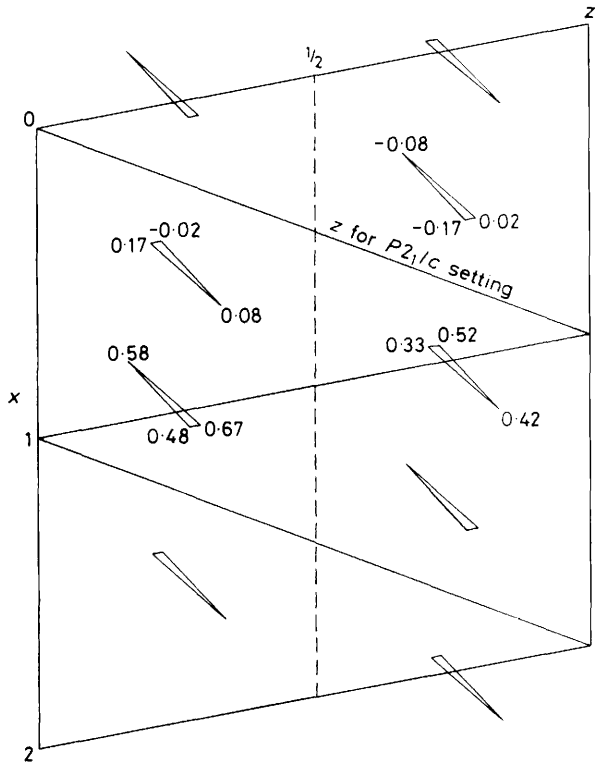

Figure 1. Projection of the structure of $[Ru_3(CO)_{12}]$ down the two-fold screw axis. Only the metal skeleton is shown. Note the alternative unit cells for $P2_1/n$ and $P2_1/c$; the sense of the axes is changed so that $\beta > 90°$ for either

Equally, well resolved bands in the various b_u spectra are not too badly at variance (Table 2).

Description of Crystal Structure.—Dodecacarbonyl-*tri-angulo*-tri-ruthenium(0) [and -osmium(0)] crystallise in the space group C_{2h}^5, with four molecules per unit cell, in general sites of no formal symmetry.[3] The conventional setting for this space group is $P2_1/c$, but the crystal morphology relates more easily to the alternative $P2_1/n$. The structure is shown in projection down the two-fold axis in Figure 1, where the relation between the two settings is made clear.

Although the molecules and the crystal have low formal symmetry, the arrangement of non-centrosymmetric, planar based molecules into a centred structure implies that the planes must be parallel throughout. In addition, one of the M–M vectors is nearly parallel to the crystal two-fold axis. This

Table 1. Intensities (arbitrary units) and frequencies (cm^{-1}) for single-crystal $[Ru_3(CO)_{12}]$ Raman spectra using molecular axes

	Crystal axes	ll	ss	*yy*	*xz'*	s*y*	ls	l*y*		Direct	By contiguity, or reference to solution	Mean	Solution value
	C_{2h}^5 species	a_g	a_g	a_g	a_g	b_g	a_g	b_g		assignment	data D_{3h}	frequency	(ref. 7)
	Molecule axes	*zz*	*xx*	*yy*	*	*xy*	*xz*	*zy*					
	Ideal D_{3h} species	a_1'	$a_1' + e'$	$a_1' + e'$	a_1'	*e'*	*e''*	*e''*	C_{2h}	D_{3h}			
a	1 950w	—	—	2	0	—	—	—	a_g	?			
b	1 976.7	—	—	0	0	1	—	2	b_g		*e''*–*e''*	1 979.4	*e''* 1 944.5
c	1 979.3	2	4	11	0	—	9	—	a_g				
d	1 982.2	0	0	0	0	3	—	22	b_g	*e''*			
e	1 987.1	0	24	68	1	—	6	0	a_g	*e'*			
f	1 990.3	0	—	0	0	8	—	0	b_g	*e'*	*e'*	1 995.2	*e'* 2 012.5
g	1 994.1	5	—	23	0	0	4	—	a_g		a_2'	1 994.1	a_2' 1 999.5
i	1 997.5	5	24	73	1	—	25	0	a_g	*e'*			
j	2 005.7	0	—	0	0	24	—	7	b_g	*e'*			
k	2 012w	—	—	0	0	†	—	†	b_g		*e'*		
l	2 016w	—	—	1	0	†	—	†	a_g?		*e'*	2 016.4	*e'* 2 018.7
m	2 021.2	2	—	0	0	36	5	3	$a_g + b_g$	*e'*			
n	2 025.0	35	11	18	39	—	—	—	a_g		a_2''	2 025.0	a_2'' 2 031.3
o	2 026.6	—	—	—	—	8	—	—	b_g			2 027.7	a_1' 2 036.0
p	2 028.7	78	122	44	90	—	6	—	a_g	a_1'	a_1'		
q	2 042w	—	—	†	0	†	—	†	b_g?		*e'*		
r	2 051w	—	†	1	1	†	—	—	a_g?		*e'*	2 056	*e'* 2 061.2
s	2 063w	†	—	2	2	—	—	—	a_g		*e'*		
t	2 066w	—	—	1	0	—	—	†	b_g?				
u	2 119.3	70	60	30	5	—	8	—	a_g	a_1'		2 119.3	a_1' 2 120.0

* Approximate $(x + z)(x - z)$. Dashes indicate probable zero intensities obscured by overlapping peaks or orientation impurity. Daggers (†) are intensities of less than 0.5 on the arbitrary scale in use. Square braces ([]) indicate split degeneracies and curly braces ({}) indicate correlation doublets.

Table 2. $[Ru_3(CO)_{12}]$ single-crystal i.r. spectra in reflectance (cm^{-1}) *

Crystal	μ_y	μ_x	μ_s	μ_l		Assignment	
C_{2h}^5 species	a_u	b_u	b_u	b_u			
Molecule	*y*	*x* + *z*	*x*	*z*			
Ideal D_{3h} species	*e'*	*e'* + a_2''	*e'*	a_2''	Mean	C_{2h}^5	D_{3h}
		1 977 (1)		1 977 (13)	1 977	b_u	*e''*
	1 981 (8)				1 981	a_u	*e''* † *e''*
		1 986 (8)	1 985 (5)	1 987 (30)	1 986	b_u	*e'*
	1 993.5 (3)				1 994	a_u	a_2' *e'*
	1 999 (45)				1 999	a_u	
		1 999.5 (35)	2 001 (15)	1 999 (30)	2 000	b_u	
	2 017 (20)				2 017	a_u	*e'*
			2 018 (15)	2 015 (40)	2 017	b_u	
		2 021 (15)	2 022 (15)	obscured	2 022	b_u	*e'*
	2 027.5 (20)				2 028	a_u	
		2 030 (35)		2 025 (s br)	2 030	b_u	a_2''
	2 034 (25)				2 034	a_u	a_1'
		2 047 (s br)		2 044 (s br)	2 046	b_u	
	2 055 (20)				2 055	a_u	*e'*
			2 063 (s br)		2 063	b_u	
	2 067 (s br)				2 067	a_u	*e'*
		2 088 (20)	2 084 (20)		2 086	b_u	? ↕ 2 075 ?
	2 119	(Absorption spectrum only)			2 119		a_1'

* Intensities are in parentheses. Square braces ([]) indicate split degeneracies and curly braces ({}) indicate correlation doublets. The double-headed arrow represents a Fermi resonance. † Correlation doublet or split degeneracy.

arrangement makes it particularly straightforward to relate crystal measurements to molecular axes. This fortunate circumstance was further aided by the realisation that the non-symmetry determined birefringence, for light propagating parallel to the two-fold axis, is in fact determined, at least for visible light, by the molecular planes. It was thus possible to use this ' inadvisable ' crystal orientation for Raman spectroscopy, and to obtain measurements using the molecular D_{3h} axes directly. For convenience, the *y* axis for the molecule was chosen to coincide with the monoclinic two-fold axis, also *y* in crystallographic convention.

It may be helpful to note that the structure can be regarded as derived from an ideal $D_{2h}^{25} = I_{mmm}$ arrangement by a shear deformation.

Crystal Morphology.—Morphological examination quickly identifies the two-fold or *y* axis, and shows that the best developed faces are {010} and {001} of the $P2_1/n$ setting. In practice slightly elongated plate-shaped crystals are usually found, in which either may be the main face; they are easily distinguished by detailed morphology and birefringence. The {010} platelets are typically elongated along *x*, with {*mn*0} end

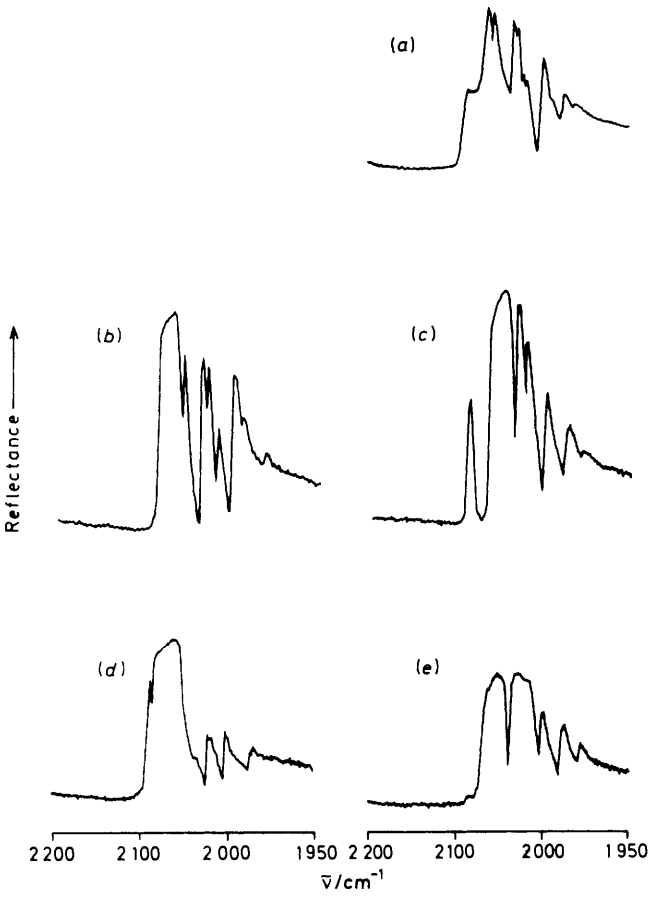

Figure 2. Single-crystal i.r. reflectance spectra for $[Ru_3(CO)_{12}]$: (*a*) {001} face, unpolarised light; (*b*) {001} face, μ_y or a_u spectrum; (*c*) {001} face, crystal μ_x = molecular $\mu(x + z)$, b_u spectrum; (*d*) {010} face, μ_s = molecular μ_x, b_u spectrum; (*e*) {010} face, μ_l = molecular μ_z, b_u spectrum

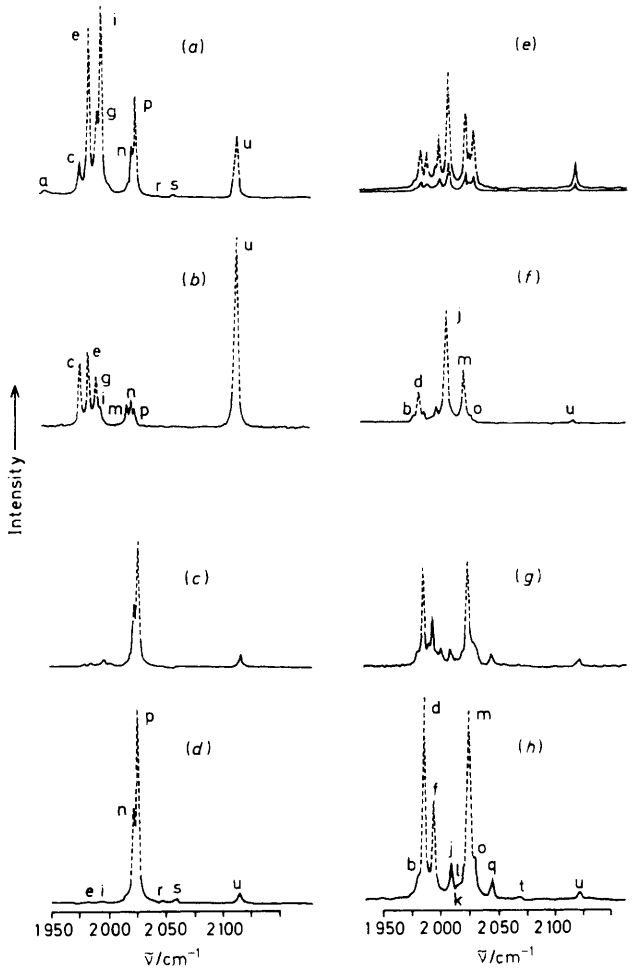

Figure 3. Single-crystal Raman multiplex spectra for some orientations of $[Ru_3(CO)_{12}]$. These measurements use the *crystallographic* ($P2_1/n$) *x* and *y* (= 2_1) axes, with *z'* perpendicular to both: (*a*) *z'* (*yy*) *z'* (Porto notation [2]); (*b*) *z'* (*xx*) *z'*, × 2 (approx.); (*c*) *z'* (*xz'*) *x*, × 0.6 (approx.); (*d*) *z'* (*xz'*) *x* optimised, × 0.9 (approx.) [(*a*), (*b*), and (*d*) encompass crystal a_g modes]; (*e*) *z'* (*yz'*) *x*, × 0.9 and × 2.5 (approx.); (*f*) *z'* (*yz'*) *x* optimised, × 2.5 (approx.); (*g*) *z'* (*yx*) *z'*, × 1.8 (approx.); (*h*) *z'* (*yx*) *z'* optimised, × 4 (approx.) [(*f*) and (*h*) encompass crystal b_g modes]

bevels. They are parallelogram shaped and extinguish a little off the diagonal; in fact parallel and perpendicular to (10$\bar{2}$) of $P2_1/n$ within experimental error, which is as stated, the M_3 plane. These were the crystals used to take the ' direct ' molecular measurements. In Tables 1 and 2 these extinction directions are labelled ' l ' and ' s ' for the ' long ' and ' short ' diagonal, corresponding respectively to molecular *z* and *x* axes (*z* is C_2 axis of D_{3h}).

The {001} platelets, representing a more extensive development of the major side faces of the {010}, are typically an elongated hexagon with the two-fold axis along the short dimension. The hexagonal ends are then the terminations of the bevels previously referred to.

Experimental

Raman Spectra.—For the single-crystal and powder Raman spectra, the He/Ne laser and the multiplex detector [1] were used with a 0.7-m spectrograph (1 800 lines per mm holographic grating; one half of a Spex 1401D). The same ethyl violet filter solution was used, again limiting spectra to >800 cm^{-1} shift from the He/Ne exciting line. Calibration was performed using plasma lines as previously.[1] In this connection, we noted a tendency for the grating to drift into its drive backlash when not being scanned, and would recommend installing a light spring loading to prevent this. In the event, this equipment was not available for the whole of the study, and final calibration was performed on a Cary 82 scanning Raman spectrometer used for later spectra. Resolution for the multiplex spectra was better than 1 cm^{-1} in this case, and the good signal-to-noise ratio allowed detection of weak bands previously seen only at 15 K and with scans of over 1 h.[6]

For a Raman collection system of finite aperture, there is a finite term defining collection of light not originating from the required Raman tensor element.[2] This term is generally compounded by stray areas of polycrystalline material, and internal reflections from the faces of small crystals. Using the Tracor data manipulation facility, it was possible to subtract out these orientation impurity effects, and the three less intense (and therefore more susceptible) orientations are treated in this way in Figure 3(*d*), (*f*), and (*h*).

Crystals of up to a few mm dimensions were chosen for their optical clarity and good extinction properties.

Measurements were made at angles of 0 or 90° to the exciting laser beam as convenient; in the former case the directly

transmitted laser beam was intercepted on a beam stop with the loss of a few percent of the Raman signal.

Infrared Spectra.—A commercial Specular Reflectance accessory (Perkin-Elmer) was used with a PE model 580B i.r. spectrometer. As mentioned above, a micro-reflectance unit was also tried, but the convergence effects proved troublesome. Since no atmospheric absorptions occur in the range investigated, it was not necessary to use a second unit in the reference beam.

For the i.r. spectra, crystals were selected for size and facial development; perfection is not important. Several crystals were mounted together on a non-reflective substrate.

Results

The results for the pertinent directions are presented in Table 1 (Raman) and Table 2 (i.r.). The multiplex Raman spectra are shown in Figure 3, including those not used in Table 1. The scanned spectra were of poorer signal-to-noise ratio, but otherwise acceptable for all but the weakest peaks, and are all included in Table 1.

In Table 1 the relative intensities between orientations are somewhat imprecise (being notoriously difficult to assess). The peaks are labelled alphabetically to facilitate comparison with Figure 3.

The i.r. spectra are shown in Figure 2. The {001} face spectra are similar to some previous results of Adams and Taylor,[5] although they appear to have incorrectly assigned the electric vector direction. We have also made cautious use of {010} face data, and as with the Raman, this requires some justification. The birefringence for this face is not fixed by the crystal symmetry, with the result that sudden changes could, in principle, occur with wavelength, particularly in regions of high absorbance. However, both vector directions excite crystal b_u modes, so that the only likely problem is the appearance of polarisation artefacts; intensity data should be approximately correct and meaningful. Two checks were made. (i) Spectra were run with a pre-sample polariser, as well as an analyser in position. The differences were minimal after allowing for the variable throughput of the (polythene) pre-polariser. (ii) The b_u band positions were not different by more than a few cm^{-1}, where the same bands appeared in different orientations.

It thus appears that the molecular axes retain sufficient importance in the crystal to allow the use of the {010} faces in the i.r. as well as the visible region.

Discussion

The correlations between the C_{2v} corner units or moieties and the D_{3h} molecule have been dealt with in Part 1,[1] together with any imposed limitations on the form of the Raman tensor. In the crystal, the number of bands observed clearly indicates that the expected [5-7] correlation doubling and splitting of degeneracy both appear to some extent. In addition, the D_{3h} Raman-inactive bands may appear. The sensitivity for crystal spectra is much greater than for solutions, not only because of greater number density, but also because of orientation/polarisation discrimination. The degeneracies unfortunately split in arbitrary orientation, since the site has no symmetry.

Table 1 shows immediately that the molecular *yy* Raman spectrum, which should under D_{3h} be the same as the *xx*, is in fact somewhat more complex. This we take to be due to more severe mixing under the influence of the crystal symmetry axis; accordingly the simpler *xx* spectrum is used for assignment purposes.

Assignments were made on the following criteria (see Table 1).

(*i*) Only molecular a_1' modes have a *zz* component; the second a_1' mode is thereby easily assigned at 2 028.7 cm^{-1} (band p), with a position corresponding well to the solution value. The assignment is confirmed by the appearance of band p strongly in the crystal *xz'* spectrum [molecular $(x + z)(x - z)$], which also shows that *zz* and *xx* components are of opposite sign, corresponding well with the expected radial–axial out-of-phase character, and the high value of depolarisation ratio observed in solution (*cf.* Part 1).[1] The assignment of the 2 119 cm^{-1} high-frequency band to the in-phase totally symmetric frequency was never in doubt, and is here confirmed.

(*ii*) Remaining bands with molecular *xx* components should be of *e'* origin; these may also have *xy* components, or they may alternatively be coupled with separate *xy* bands, depending on the orientation in which the degeneracy has split. Band n was *not* so assigned, since the appearance of strong *zz* and crystal *xz'* intensity, coupled with its closeness to the a_1' origin band at 2 028.7 cm^{-1}, make it much more likely that this intensity is due to mixing. Although Fermi resonance cannot be ruled out for the origin of this band, it is more satisfactorily assigned, by reference to the i.r. results, as the a_2'' vibration which of course is allowed to mix in this way in the crystal. In this context we should also note band g, appearing with major intensity only in *yy*. This anomalous pattern was resolved by reference to the previous work of Kettle and co-workers,[7] and the band satisfactorily assigned to the ' silent ' a_2' mode.

(*iii*) A single *e''* vibration is expected (with up to four crystal components), and band d is the only one to show unambiguous concentration of intensity into the *xz* or *yz* molecular components. Bands b and c are then a perfectly acceptable pairing, leading to a firm ' low end ' assignment for modes of predominantly *e''* origin, as also found from the calculations and solution spectra.[7]

(*iv*) Remaining assignments, also shown in a second, subsidiary column in Table 1, were made by reference to contiguous assignments and solution data.[1,7] In particular, the four very weak bands q, r, s, and t, showing no decisive orientation effects, are presumed to originate from the high-frequency *e'* mode.

In summary, we note the satisfactory confirmation of a_1' and *e''* assignments for the solution species. The pattern of dominance in the anisotropic Raman solution spectrum by a single *e'* frequency, whilst somewhat broken down in the crystal, is also observed in the large summed intensities of bands e,f,i,j in the crystal (seen most clearly in the powder spectrum [6]). Band m is clearly anomalous in this context and has presumably borrowed intensity, despite its unambiguous orientation behaviour. The bands k and l, with which it is paired, remain very weak however. Bands c and d are also too intense to have been missed, at least in the higher resolution $[Os_3(CO)_{12}]$ spectrum, were the *e''* Raman intensity comparable in solution; whilst the q,r,s,t and k,l sequences show that intensity remains low for comparatively isolated frequencies. Thus the a_2''/high-frequency *e'* assignments, made originally by requiring a reasonable force field,[7] and which might have looked to Raman spectroscopy for confirmation, remain at this stage a (highly likely) hypothesis. However, further confirmation of the utility of the i.r. {010} face data (Table 2, Figure 2) comes from the failure of the a_2'' mode to appear in the molecular μ_x (crystal μ_x) spectrum, thus elegantly verifying that assignment. Mixing with the second a_1' mode, already noted for the Raman bands, also makes the best sense of the i.r. spectra.

The i.r. μ_y spectrum (crystal and molecular *y* axis) is as

disappointing as the Raman *yy* spectrum; once again we propose more widespread mixing and intensity borrrowing occurring under the influence of the crystal symmetry axis. Equally disappointing in the i.r., the *e'* modes appear strongly in all orientations.

The assignments proposed in Table 2 are internally consistent, although it is clear that the Raman spectra show weak bands better, and are also better resolved. These limitations arise from the nature of reflectance spectroscopy, whilst the less satisfactory orientation information in the i.r. is unexpected. Accordingly, both Raman and solution data [1,7] were needed to assist in the assignments of Table 2.

Conclusions

We believe that the assignments of Kettle and co-workers [7] and of Adams and Taylor,[5] whilst similar to ours, suffer some defects. In particular, Adams and Taylor propose two unreasonably large correlation splittings. (A simple list of Raman–i.r. near coincidence is enough to demonstrate that correlation splittings are generally small.) This we avoid by the assignment of 2 086 cm^{-1} to a Fermi resonance component * (it is only surprising more are not seen), and by a slight reassignment in the 2 030 cm^{-1} region. The latter meets Kettle's objection to his own a_2'' assignment, in a more satisfactory way than Adams. As we have noted, the a_2'' assignment is in fact particularly clear cut from the {010} face i.r. intensities. We also find it impossible to believe that natural ^{13}C substitution in a twelve-carbonyl molecule [5] could possibly produce the observed weak but quite *sharp* bands at around 1 980 cm^{-1}; the solution–solid shift when these are assigned to the e'' mode is perfectly reasonable for the low-frequency end of the spectrum. These shifts are summarised in Table 1.

Finally, it must be emphasised that these descriptions are approximate only; many of the pure modes of origin in the undistorted molecule clearly undergo substantial mixing in the crystal. This is evidenced by the far from ideal intensity distributions observed.

It is clear that this study, although time-consuming, has added to our knowledge in terms of the aims outlined. Thus the solution assignments were aided in a number of ways. The oriented gas-phase approximation was not rigorously applicable, but sufficient vestiges of it remained to be useful, particularly in the Raman effect. Generalisations must await further work on other carbonyls.

* Or it could be assigned to a reflectance anomaly, since it is not apparently observed in absorption (alone amongst the well defined reflectance features). For a Fermi resonance, the lowest-frequency molecular modes (60—100 cm^{-1}) plus low-frequency carbonyl modes (1 977—2 017 cm^{-1}) supply several candidates.

Acknowledgements

See preceding paper.

References

1 Part 1, T. R. Gilson, preceding paper.
2 See, for example, T. R. Gilson and P. J. Hendra, ' Laser Raman Spectroscopy,' Wiley, Chichester, 1970.
3 M. R. Churchill, F. J. Hollander, and J. P. Hutchinson, *Inorg. Chem.*, 1977, **16**, 2655.
4 J. C. Decius and R. M. Hexter, ' Molecular Vibrations in Crystals,' McGraw-Hill, 1977.
5 D. M. Adams and I. D. Taylor, *J. Chem. Soc., Faraday Trans. 2*, 1982, 1561.
6 S. Kishner, P. J. Fitzpatrick, K. R. Plowman, and I. S. Butler, *J. Mol. Struct.*, 1981, **74**, 29.
7 G. A. Battiston, G. Bor, U. K. Dietler, S. F. A. Kettle, R. Rosetti, G. Sbrignadello, and P. L. Stanghellini, *Inorg. Chem.*, 1980, **19**, 1961.

Received 16*th May* 1983; *Paper* 3/797